PRAMANA
— journal of
physics

Vol. 61, No. 1
July 2003
pp. 131–139

Comparison of resonant tunneling in AlGaAs/GaAs parabolic and diffusion modified quantum wells

SUDHIRA PANDA, B K PANDA and S FUNG*
Institute of Physics, Sachivalaya Marg, Bhubaneswar 751 005, India
*Department of Physics, University of Hong Kong, Hong Kong, People's Republic of China
Email: sudhira@iopb.res.in; bpanda@iopb.res.in

MS received 23 December 2002; revised 25 March 2003; accepted 1 April 2003

Abstract. Double barrier resonant tunneling diode using annealing induced diffusion modified quantum well is proposed as a viable alternative to that using parabolic quantum well which requires complex techniques to fabricate it. The transmission coefficients are calculated using the hybrid incremental airy function plane wave approach. The room temperature current–voltage characteristics have been calculated using transmission coefficients. The current–voltage characteristics are found to be similar in both diodes.

Keywords. Parabolic and diffused resonant tunneling diodes; transmission coefficient; current–voltage characteristics; dark current.

PACS Nos 73.40.G; 66.30.Ny; 85.35.B

1. Introduction

Rapid advances in semiconductor deposition technology using molecular beam epitaxy (MBE) method has led to the realization of different quantum well structures with rectangular [1], parabolic [2–5] and triangular [6] confinement profiles. The diffusion modified quantum well is fabricated by annealing rectangular quantum well (RQW) under suitable conditions [7–10].

Since the pioneering work of Tsu and Esaki [11], the resonant tunneling diode (RTD) in the quantum well structure has been intensively studied both theoretically and experimentally over the last three decades. These diodes are also useful for perpendicular transport at ambient temperatures [12]. The early $J-V_{\mathrm{a}}$ measurements of the RTD are explained using Chang–Esaki–Tsu (CET) model [13]. More accurate measurements [14] show bistability and plateau-like structures which exist at a bias voltage away from the resonance bias voltage. Recently these structures are found to arise from the coupling between energy levels in the emitter quantum well and main quantum well [15].

Although most of the studies have been concentrated on the RQW structures [16], there have been a few attempts to study this in the parabolic quantum well (PQW) and triangular quantum well-based RTDs. The reason behind this is that the fabrication of a RTD with

PQW is more involved compared to that in the RQW. In the parabolic RTD the peaks of the current densities in experiments are evenly spaced due to equally placed sub-bands in it [3,5]. Using CET model, Tan *et al* [17] have studied the resonant tunneling in the PQW and found that the current densities in this well are peaked at larger applied voltages compared to rectangular RTD due to stronger confinement of the energy levels in it.

Li [18] has theoretically shown that the annealing induced diffusion modified quantum well (DMQW) can also show a parabolic-like confinement profile under some suitable conditions. As a result of this the third-order susceptibilities are similar in both PQW [19] and DMQW [18]. It is therefore worth comparing current densities in RTDs based on PQW and DMQW. We employ CET model for calculating current densities in spite of its limitations in finding bistability and plateau-like structures. We neglect current densities arising from the phonon [20] and plasmon assisted processes [21].

In §2, we present structures of RTDs for both PQW and DMQW. In §3, we present a general scheme for calculating transmission coefficients in PQW and DMQW-based RTDs. In §4, the current densities as a function of the applied voltages are shown. The dark current densities are calculated in §5 and finally the paper is concluded in §6.

2. Potential profiles

2.1 *Parabolic well structure*

The RTD with parabolic potential profile can be fabricated using two different techniques by the MBE method. In one method the parabolic well is fabricated by depositing alternate layers of GaAs and AlGaAs in such a way that the average Al-concentration in the well is parabolically graded by adjusting the ratio of the layer thicknesses [2,5]. In the second method the material composition of the well is changed quadratically with position to obtain PQW [3]. Both these methods require accurate deposition techniques.

The potential profile for the PQW is generally constructed using position independent force constant and the energy levels are calculated using constant effective mass [19]. However, the Al concentration in this well varies quadratically with the well width resulting in position-dependent effective mass. For this reason we have followed the scheme of Tan *et al* [17] for describing the potential profile of a parabolic well. In their method the position-dependent Al atomic fraction is expressed as

$$x(z) = \frac{4x_0}{L_1^2}\left(\frac{L_1+2L_2}{2} - z\right)^2, \tag{1}$$

where L_1 and L_2 are well and barrier widths respectively. The heterostructure under applied bias is described as

$$V(z) = \begin{cases} 0 & \text{for } z < 0, \\ V_d(z) - eFz & \text{for } 0 \le z \le L, \\ -eV_\mathrm{a} & \text{for } z > L \end{cases} \tag{2}$$

where $L = L_1 + 2L_2$ and $F = V_\mathrm{a}/L$ with V_a being the applied voltage.

The confinement profile $V_\mathrm{d}(z)$ is calculated as

$$V_\mathrm{d}(z) = 0.7[E_\mathrm{g}\{x(z)\} - E_\mathrm{g}\{x(0)\}]. \tag{3}$$

The position-dependent effective mass is calculated as $m^*(z) = m^*(x(z))$. The Al concentration dependent band gap and effective mass are taken from ref. [1].

2.2 *Diffusion modified quantum well*

As mentioned earlier, the rapid annealing of the as-grown RQW produces DMQW. At the growth temperature, generally, there are not enough Ga vacancies, but only excess arsenic. It is only during subsequent annealing at high temperature (850 °C) that this arsenic dissolves into lattice producing Ga vacancies which are free to diffuse. The Al atoms diffuse into GaAs region and occupy Ga vacancies. It has been found that the intermixing is enhanced when the GaAs well is grown at low temperature [22]. The extent of Al diffusion is characterized by diffusion constant L_d which is defined as $L_\mathrm{d} = \sqrt{Dt}$ where D and t are diffusion constant and annealing time respectively. The annealing needs the quantum well to be capped by some capping material in the front and back surfaces. Silicon nitride is chosen as it has been found to give the lowest diffusion coefficient for intermixing in the emitter and collector regions below the silicon nitride capping layers.

Taking isotropic diffusion constant, the concentration profile $x(z)$ has been derived as

$$x(z) = x_0 \left[1 - \frac{1}{2} erf\left(\frac{z - L_2}{2L_\mathrm{d}}\right) + \frac{1}{2} erf\left(\frac{z - L_1 - L_2}{2L_\mathrm{d}}\right)\right]. \tag{4}$$

The potential profile of the RTD is expressed in the same way as in eq. (2) with V_d calculated using eq. (3).

In order to design the DMQW with equally spaced eigenstates, the structural parameters and the interdiffusion length of the DMQW are chosen very carefully so that the confinement profile is parabolic-like in shape. In figure 1 we have compared potential profile of the parabolic and diffused RTDs. As can be seen, the potential profile of the DMQW nearly matches with the parabolic profile with a slight disagreement at the barrier regions.

3. Transmission coefficients

The effective mass equation for describing the RTD is given by

$$\left[-\frac{\hbar^2}{2}\frac{\partial}{\partial z}\frac{1}{m^*(z)}\frac{\partial}{\partial z} + V(z)\right]\Psi_E(z) = E\Psi_E(z), \tag{5}$$

where $\Psi_E(z)$ is wave function at energy E.

The solution of this equation for the region $z < 0$ is given by the incident and reflected plane waves [23,17]

$$\Psi_E(z) = A_2 \mathrm{e}^{ik_0 z} + B_2 \mathrm{e}^{-ik_0 z}, \tag{6}$$

where $k_0 = \sqrt{2m^*(0)E/\hbar^2}$. Similarly for the region $z > L$, the solution is given only by the propagating plane wave as the electron is not reflected in this region,

$$\Psi_E(z) = A_1 \mathrm{e}^{ik_t z}, \tag{7}$$

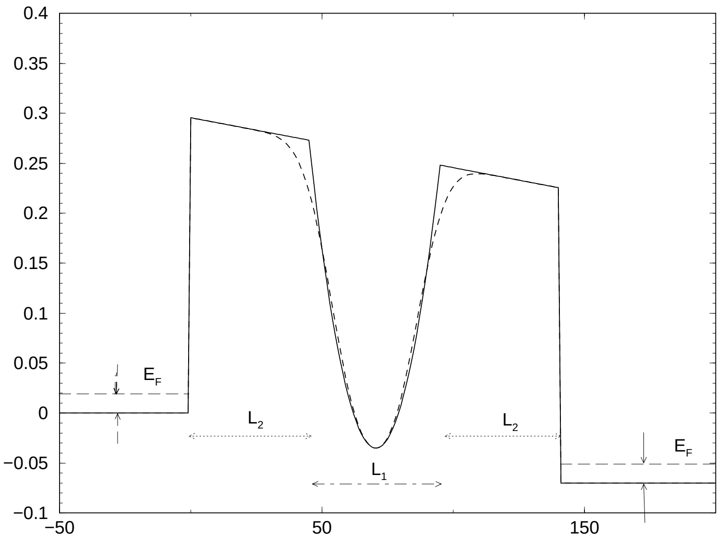

Figure 1. Comparison of the potential profiles of parabolic and diffused AlGaAs/GaAs double barrier resonant tunneling diodes. The parameters used for the parabolic well are $L_1 = 50$ Å, $L_2 = 45$ Å and $x = 0.3$ while those for the diffused well are 52 Å, 35 Å and 0.3175 respectively. The diffusion length L_d for the diffused well is 6 Å.

where $k_t = \sqrt{2m^*(0)(E + eV_\mathrm{a})/\hbar^2}$. The transmission coefficient is defined as [23]

$$T(E) = \sqrt{\frac{E + eV_\mathrm{a}}{E}} \frac{A_1}{|A_2|^2}. \tag{8}$$

For evaluating the transmission coefficient it is required to find A_1 and A_2. A_1 can be arbitrarily chosen so that it is multiplied with A_2. Since we are taking the ratio of A_1 and A_2, the transmission coefficient is independent of the choice of A_1. In our case we have taken $A_1 = 1$.

We have followed the hybrid incremental airy function approach of Tan *et al* [17] with some modifications in order to solve eq. (5) in the region $0 \le z \le L$ for both PQW and DMQW. The potential profile is sub-divided into a number of strips (N). Before applying the electric field the potential within each strip is assumed to have rectangular barrier with constant height. The effective mass is also assumed to be constant within a strip. Under applied bias, the slope of each strip changes according to the external voltage drop across the strip. It is important to choose an appropriate width of the strip in order to obtain converged results. For N strips, the width of each strip is given by $\Delta = L/(N-1)$. We vary N to find the convergence in the transmission coefficient. The barrier of the ith rectangular strip is set at $z_i = L - (i-1)\Delta$. The solution of the effective mass equation for the ith strip is given by

$$\Psi_E(z_i) = C_i Ai(X_i) + D_i Bi(X_i), \tag{9}$$

where Ai and Bi are airy functions [24]. The dimensionless coordinate X_i is defined as

$$X_i = -\left[\frac{2m^*(z_i)}{(e\hbar F)^2}\right]^{1/3} \left\{E - V_{\mathrm{d}}(z_i) + eFz_i\right\}. \tag{10}$$

Using current continuity equations, C_1 and D_1 are obtained as

$$C_1 = \pi \mathrm{e}^{ik_0L} \left[Bi'(X_1^-) + iBi(X_1^-)\frac{(m_1^-)^{2/3}}{m(0)}\left(\frac{\hbar^2}{2eF}\right)^{1/3} k_t\right], \tag{11}$$

$$D_1 = -\pi \mathrm{e}^{ik_0L} \left[Ai'(X_1^-) + iAi(X_1^-)\frac{(m_1^-)^{2/3}}{m(0)}\left(\frac{\hbar^2}{2eF}\right)^{1/3} k_t\right], \tag{12}$$

where the dimensionless coordinate is defined as

$$X_i^{\pm} = -\left[\frac{2m(z_i \pm \Delta/2)}{(e\hbar F)^2}\right]^{1/3} \left\{E - V_{\mathrm{d}}\left(z_i \pm \frac{\Delta}{2}\right) + eFz_i\right\}. \tag{13}$$

The average potential and effective mass in each strip is chosen at the center of the strip. The coefficients for C_i and D_i from 2 to N are calculated using the continuity conditions at z_i boundaries in the following way:

$$\begin{aligned}
&\begin{pmatrix} Ai(X_i^-) & Bi(X_i^-) \\ Ai'(X_i^-)/(m_i^-)^{2/3} & Ai'(X_i^-)/(m_i^-)^{2/3} \end{pmatrix} \begin{pmatrix} C_{i+1} \\ D_{i+1} \end{pmatrix} \\
&= \begin{pmatrix} Ai(X_i^+) & Bi(X_i^+) \\ Ai'(X_i^+)/(m_i^+)^{2/3} & Ai'(X_i^+)/(m_i^+)^{2/3} \end{pmatrix} \begin{pmatrix} C_i \\ D_i \end{pmatrix}.
\end{aligned} \tag{14}$$

Using the computed values of C_{N+1} and D_{N+1}, we find A_2 as

$$\begin{aligned}
A_2 = {}& \frac{1}{2}\left[C_{N+1}Ai(X_N^+) + D_{N+1}Bi(X_N^+)\right] + \frac{i}{2}\left[C_{N+1}Ai'(X_N^+) + D_{N+1}Bi'(X_N^+)\right] \\
&\times \left[\left(\frac{2eF}{\hbar^2}\right)^{1/3} \frac{m(0)}{(m_N^+)^{2/3}} \frac{1}{k_0}\right].
\end{aligned} \tag{15}$$

In figure 2, we have shown transmission coefficients for both RTDs at various applied bias. As can be seen, they are quite similar.

4. Current density

The current density J at temperature T can be calculated using the expression [16]

$$J(V_{\mathrm{a}}) = \frac{em^*(0)k_{\mathrm{B}}T}{2\pi^2\hbar^3} \int_0^{\infty} T(E) \ln\left(\frac{1 + \exp[(E_{\mathrm{F}} - E)/k_{\mathrm{B}}T]}{1 + \exp[(E_{\mathrm{F}} - E - eV_{\mathrm{a}})/k_{\mathrm{B}}T]}\right) \mathrm{d}E, \tag{16}$$

where E_{F} is the Fermi energy which is calculated by equating the fully ionized donor concentration with the occupied sub-band states of the quasi two-dimensional electron gas.

The $J - V_{\mathrm{a}}$ characteristics of both RTDs are shown in figure 3. We find that the current densities of both RTDs are quite similar which suggest that a carefully designed diffused RTD can be a compliment for parabolic RTD.

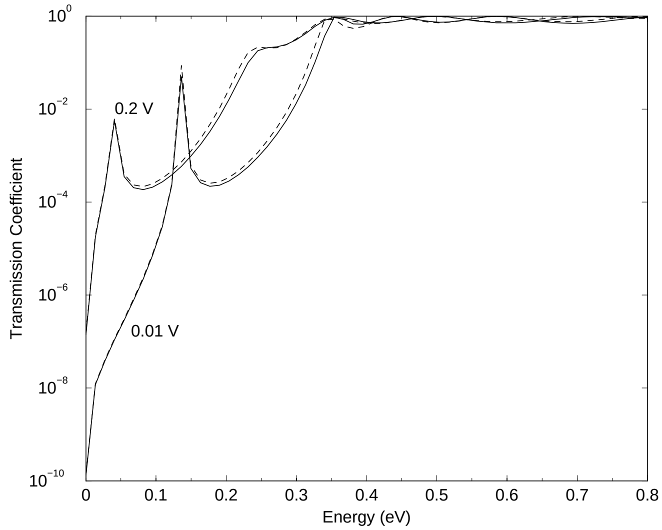

Figure 2. Comparison of the transmission coefficients for the parabolic and diffused RTDs at different applied bias.

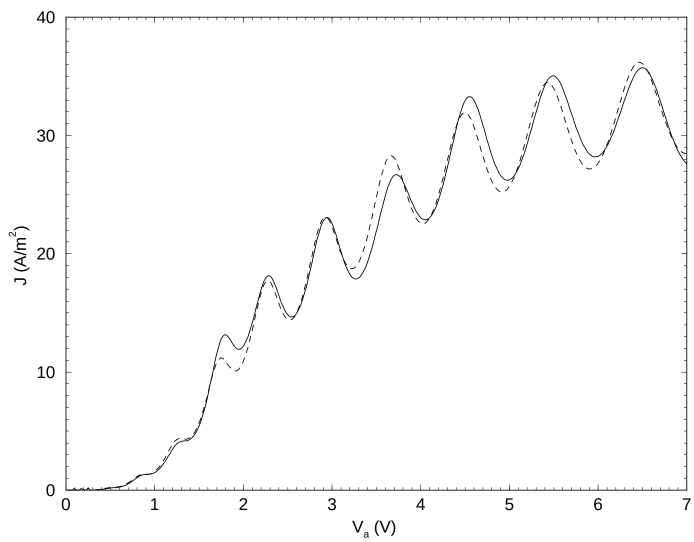

Figure 3. Comparison of the $J-V_{\mathrm{a}}$ characteristics for the parabolic and diffused RTDs at different applied bias.

5. Dark current

The dark current due to the thermionic emission current is given by [25]

$$J_{\mathrm{dark}}(V_{\mathrm{a}}) = ev_{\mathrm{d}} \int_0^{\infty} N_{2d}(E, V_{\mathrm{a}}) T_c(E, V_{\mathrm{a}}) f(E) \mathrm{d}E, \tag{17}$$

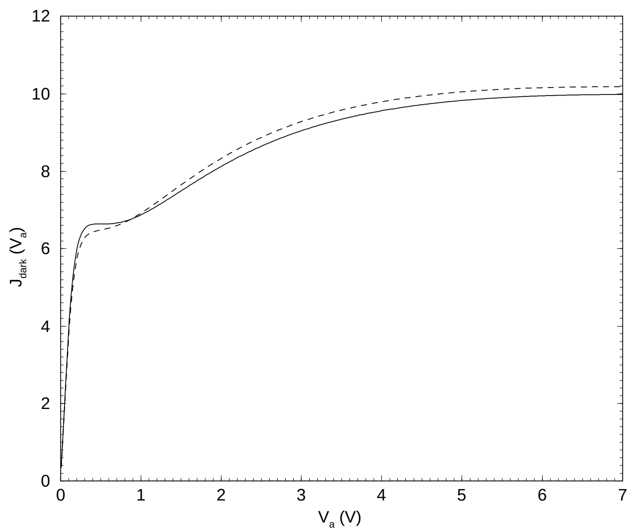

Figure 4. Comparison of the dark current densities for the parabolic and diffused RTDs at different applied bias.

where N_{2d} is the two-dimensional density of states [26] and $f(E)$ is the Fermi–Dirac distribution function. T_c is the probability of tunneling through the barrier in the direction of the electric field. We have used WKB approximation [27] for calculating T_c. Both T_c and N_{2d} are calculated taking position dependence of the effective mass and then integrating over well-width. The drift velocity $v_{\rm d}$ is given by [28]

$$v_{\rm d} = \frac{\mu F}{[1+(\mu F/v_{\rm s})^{2.6}]^{1/2}}, \tag{18}$$

where μ is the mobility of electrons and $v_{\rm s}$ is the saturation velocity. In our calculation we have taken $\mu = 8000$ cm^2 V^{-1}/s and $v_{\rm s} = 2\times 10^7$ cm/sec from ref. [26]. The calculated dark current densities for RTDs based on PQW and DMQW are shown in figure 4. As in the resonant current densities, the dark currents are also similar in these RTDs. Compared to the resonant current densities, the dark currents are low.

6. Conclusions

In summary, we propose the DMQW as a viable alternative to the PQW. The resonant tunneling diodes prepared from these wells with similar confinement potentials show similar transmission coefficients and $J-V_{\rm a}$ characteristics. The calculated dark currents are at an acceptable level for device fabrication. Although we have prepared a set of parameters for PQW and DMQW to show similar $J-V_{\rm a}$ characteristics, there could be many such similar RTDs with similar behavior.

Unfortunately there is only one experimental work [29] which measures Stark shifts in the DMQW. The lack of experimental works on RTD based on AlGaAs/GaAs heterojunction did not allow us to determine the correctness of our results. For making a RTD based on DMQW, it is necessary to focuss our attention on several important aspects. The diffusion coefficient is invariably a function of temperature, $D = D_0 \exp(-Q/k_B T)$, where D_0 is the diffusion constant and Q is the energy required for an atom from one stable position in the crystal to the next. At 850°C the diffusion constant is found to be 1.1×10^{-18}. For getting $L_d = 6$Å, the annealing time required is nearly one hour.

Although the AlGaAs barriers are capped by Si_3N_4 to block Al atoms diffusing into the emitter and collector *n*-type GaAs regions, there is still some probability for these regions to receive some amount of Al atoms from the barrier regions. This will not pose any problem for device fabrication since the small Al concentration will allow the conduction band edge to lie only slightly below the lowest energy state in the well [5]. The contacts can be prepared by depositing and annealing AuGe/Ni/Au alloy on both sides of the device [5].

Acknowledgement

One of us Sudhira Panda acknowledges financial support from the Department of Science and Technology project SR/FTP/PS-26/2000 to carry out this work.

References

[1] Sudhira Panda, *Quantum confined Stark effect and optical properties in quantum wells*, Ph.D. thesis (University of Hong Kong, Hong Kong, 1999)
[2] R C Miller, A C Gossard, D A Kleinman and O Munteanu, *Phys. Rev.* **B29**, 3740 (1984)
[3] S Sen, F Capasso, A C Gossard, R A Spah, A I Hutchinson and S N G Chu, *Appl. Phys. Lett.* **51**, 1428 (1987)
[4] S Y Chou and J S Harris Jr., *Appl. Phys. Lett.* **52**,1422 (1988)
[5] K D Maranowski and A C Gossard, *J. Appl. Phys.* **88**, 172 (2000)
[6] A C Gossard, W Brown, C L Allyn and W Wiegmann, *J. Vac. Sci. Technol.* **20**, 694 (1982)
[7] L L Chang and A Koma, *Appl. Phys. Lett.* **29**, 138 (1976)
[8] T E Schlesinger and T Kuech, *Appl. Phys. Lett.* **49**, 519 (1986)
[9] K Mukai, M Sugawara and S Yamazaki, *Phys. Rev.* **B50**, 2273 (1994)
[10] O M Khreis, W P Gillin and K P Homewood, *Phys. Rev.* **B55**, 15813 (1997)
[11] R Tsu and L Esaki, *Appl. Phys. Lett.* **22**, 562 (1973)
[12] V V Mitin, V A Kochelap and M A Stroscio, *Quantum heterostructures – microelectronics and optoelectronics* (Cambridge University Press, 1999) ch. 8, p. 333
[13] L L Chang, L Esaki and R Tsu, *Appl. Phys. Lett.* **24**, 593 (1974)
[14] V J Goldman, D C Tsui and J E Cunningham, *Phys. Rev. Lett.* **58**, 1256 (1987)
[15] P Zhao, H L Cui and D L Wooland, *Phys. Rev.* **B63**, 75302 (2001)
[16] H Mizuta and T Tonoue, *The physics and applications of resonant tunneling diodes* (Cambridge University Press, 1995)
[17] C M Tan, J Xu and S Zukotynski, *J. Appl. Phys.* **67**, 3011 (1990)
[18] E H Li, *Appl. Phys. Lett.* **69**, 460 (1996)
[19] Y Huang and C Lien, *J. Appl. Phys.* **75**, 3223 (1994)
[20] Z W Yan, X X Liang and S L Ban, *Phys. Rev.* **B64**, 125321 (2001)
[21] C Zhang, M L F Lerch, A D Martin, P E Simmonds and L Eaves, *Phys. Rev. Lett.* **72**, 3397 (1994)
[22] J S Tsang, C P Lee, S H Lee, K L Tsai and J C Fan, *J. Appl. Phys.* **79**, 664 (1996)

[23] S S Allen and S L Richardson, *J. Appl. Phys.* **79**, 886 (1996)
[24] *Handbook of mathematical functions* edited by M Abramowitz and I A Stegun (National Bureau of Standards, Washington DC, 1964) p. 446
[25] S Ehret, H Schneider, E C Larkins and J D Ralson, *J. Appl. Phys.* **77**, 2537 (1995)
[26] T Osotchan, V W L Chin and T L Tansley, *Phys. Rev.* **B52**, 5202 (1995)
[27] A S W Lee and E H Li, *Appl. Phys. Lett.* **69**, 3581 (1996)
[28] D M-T Kuo and Y C Chang, *Phys. Rev.* **B60**, 15957 (1999)
[29] J D Ralston, W J Schaff, D P Bour and L F Eastman, *Appl. Phys. Lett.* **54**, 534 (1989)